ISSN 1027-5495. Functional Materials, 29, No.2 (2022), p. 252-262.
doi:https://doi.org/10.15407/fm29.02.252 

# Synthetic and natural flavonols as promising fluorescence probes for β-glucosidase activity screening

***O.O.Demidov*[1], *E.S.Gladkov*[1,2], *A.V.Kyrychenko*[1,2], *A.D.Roshal*[1]**

[1]Institute of Chemistry and School of Chemistry, V.N.Karazin Kharkiv National University, 4 Svobody Sq., 61022 Kharkiv, Ukraine
[2]State Scientific Institution "Institute for Single Crystals", National Academy of Sciences of Ukraine, 60 Nauky Ave., 61072 Kharkiv, Ukraine

*Received February 23, 2022*

Natural and synthetic flavonols are environmentally sensitive dyes whose emission properties are highly sensitive to their immediate environment. Here we describe the synthesis and spectral properties of flavonols bearing a series of substituents in the 4'-aryl ring. The synthesized flavonols were applied to study their capability for fluorescence sensing of β-glucosidase in physiological solutions. We found that 4'-fluoro- and 4'-carboxyflavonols revealed the essential fluorescence enhancement in the presence of β-glucosidase, which is characteristic of the protein-induced "turn-on" effect. The fluorescence titration experiments suggest that the studied flavonols favor binding to the protein, so that the probes leave a polar aqueous solution and enters a nonpolar hydrophobic environment inside a protein pocket. These findings were collaborated by molecular docking calculations, which allowed us to identify favorable binding modes and the binding affinity of the synthetic flavonols towards β-glucosidases from various sources. Molecular docking revealed the high binding affinity towards β-glucosidase, which is the same order of magnitude as the well-known natural flavonols. Our results suggest that the studied flavonol dyes can be a promising scaffold for developing novel flavonol glycosides as "turn on/off" fluorescent indicators of β-glucosidase activity.

**Keywords**: flavonol, fluorescence probe, β-glucosidase, fluorescence indicator, molecular docking.

**Синтетичні та природні флавоноли як перспективні флуоресцентні зонди для скринінгу активності β-глюкозидази**. *О.О.Демидов, Е.С.Гладков, О.В.Кириченко, О.Д.Рошаль*

Природні та синтетичні флавоноли є чутливими барвниками, емісійні властивості яких дуже чутливі до їх безпосереднього оточення. В роботі описано синтез та спектральні властивості флавонолів, що містять ряд замісників у 4'-арильному кільці. Синтезовані флавоноли були застосовані для вивчення їхньої здатності до флуоресцентного зондування β-глюкозидази у фізіологічних розчинах. Ми виявили, що 4'-фтор- і 4'-карбоксифлавоноли показали значне посилення флуоресценції в присутності β-глюкозидази, що характерно для ефекту "підсилення", що викликається білком. Експерименти з флуоресцентного титрування показують, що досліджувані флавоноли зв'язуються з білком, так що зонди залишають полярний водний розчин і входять в неполярне гідрофобне середовище всередині білкової кишені. Ці результати були об'єднані з розрахунками молекулярного докінгу, які дозволили нам визначити сприятливі шляхи зв'язування та спорідненість зв'язування синтетичних флавонолів із β-глюкозидазами з різних джерел. Молекулярний докінг виявив високу спорідненість зв'язування з β-глюкозидазою, яка знаходиться на тому ж рівні, що й відомі природні флавоноли. Наші результати свідчать про те, що вивчені барвники на базі флавонолів можуть бути багатообіцяючою основою для розробки нових глікозидів флавонолів як "підсилення/ослаблення" флуоресцентні індикатори активності β-глюкозидази.

## 1. Introduction

Flavonol-based fluorescent probes represent a class of environmentally sensitive dyes whose emission properties are highly sensitive to their immediate environment [1–7]. The notable feature of these probes is that due to the presence of a hydroxyl group at the 3-position of a flavonoid moiety they are capable of the excited-state intramolecular proton transfer (ESIPT) [8–9]. A proton transfer reaction occurs through an intramolecular hydrogen bond bridge resulting in an extremely fast ($k_{ESIPT} > 10^{12}$ $s^{-1}$) phototautomerization from normal state (N*) to tautomer state (T*) [7, 10–11]. ESIPT leads to the appearance of the dual-wavelength emission of flavonols, which is beneficial for their ratiometric fluorescence response [1, 10].

It has been shown that flavonol-based probes could be utilized as solvatochromogenic fluorophores for monitoring solvent polarity [1, 12–13] and pH [14–15], as well as the determination of water traces in organic solvents [16]. Moreover, flavonol derivatives have revealed a good sensitivity and selectivity toward metal ions in solution [7, 15, 17–20]. Their unique optical properties and biocompatibility makes flavonols a valuable template for sensing various biomolecules [21]. Flavonols show a large fluorescence "turn-on" effect upon selective binding to proteins, such as lysozymes[22] and albumins [17, 21]. The observed protein selectivity opens up the opportunity for sensing other protein binding-induced fluorescence "turn-on" [21, 23]. Flavonol-based probes are also promising fluorescent agent with a low perturbation impact on the lipid membrane physical state [24]. Due to the low molecular mass (< 500 Dalton) and low toxicity, some fluorescent flavonols have been utilized for fluorescent cell imaging [25–27].

It has recently been demonstrated that 4'-fuoroflavonol β-D-glucopyranoside can be used as a fluorescent indicator of β-glucosidase activity [28]. β-glucosidases are a group of enzymes, which catalyze the hydrolysis of aryl and alkyl β-Glucoside and cellobiose. β-glucosidase are widely spread in nature, they are present in plants, fungi, animals, bacteria and yeast also contained in the soil. In addition, these enzymes can catalyze the hydrolysis of many artificial substrates. Finally, β-glucosidases have the potential for its use in various biotechnological processes such as biofuel production and oligosaccharide synthesis. The role of β-glucosidases contained in the soil is extremely important, since they take part in the catalysis of hydrolysis and biodegradation of various β-glucosides present in plant residues. In addition, the activity and concentration of glucosidase is an indicator of soil quality [29]. The important role of β-glucosidase in various aspects of plant physiology has been reported [30]; for example, it initiates chemical protection against pathogens [31]. Regulation of glucosidase activity affects the course of Gaucher's disease [32], as well as the effectiveness of chemotherapy for breast cancer [33].

In this work, we studied binding interaction of some synthetic and natural flavonols with β-glucosidase enzyme using fluorescence titration measurements and molecular docking calculations. The fluorescence titration revealed protein- induced fluorescence "turn-on" effects for some representative flavonols, which is indicative of their binding to the hydrophobic water-free cavity of the protein. The binding mode of these ligands and other structurally similar flavonols into β-glucosidase enzymes from different sources were further identified by molecular docking.

## 2. Experimental

Flavonol synthesis. The synthesis of 2-aryl-3-hydroxy-4H-chromen-4-ones (flavonols) is well known and can be carried out in two ways: (i) as a linear synthetic strategy ("Linear" method A) with isolation and purification of an intermediate 1-(2-hydroxyphenyl)-3-phenylprop-2-en-1-ones (chalcones) [34] and (ii) as a multicomponent one-pot synthesis ("one-pot" Method B) [35]. The final step of the Algar-Flynn-Oyamada (AFO) reaction in the formation of flavonol is used in both cases (Scheme 1).

2-Aryl-3-hydroxy-4H-chromen-4-ones 1–14 may be obtained by one of the two modified methods [34–35]. The general procedures of syntheses of most typical substances of the series used in our work and typical examples of substance characteristics are given in the experimental section.

*Materials and methods.* $^{1}H$ and $^{13}C$ NMR spectra (400 and 100 MHz) were recorded on Bruker Avance 400 and Varian MR-400 spectrometers in DMSO-d6. $^{1}H$ and $^{13}C$ chemical shifts were reported relative to residual protons and the carbon atoms of the solvent (2.49 and 39.5 ppm, respectively) as the internal standard. The LCMS spectra

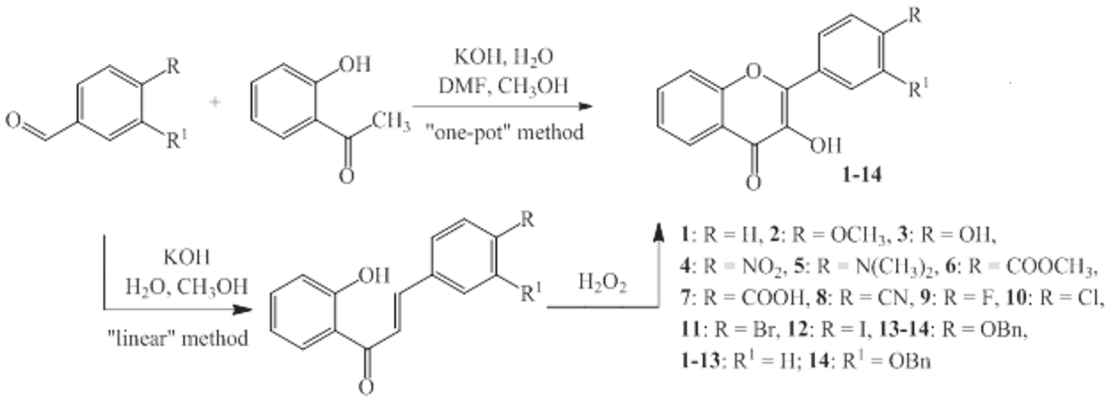


Scheme 1. Chemical structure and preparation of substituted 3-hydroxy-2-(phenyl)-4H-chromen-4-ones 1–14.

were recorded using a chromatography/mass spectrometric system that consists of a high-performance liquid chromatography Agilent 1100 Series equipped with a diode matrix and a mass selective detector Agilent LC/MSD SL, column SUPELCO Ascentis Express C18 2.7 μm 4.6 mm × 15 cm. Elemental analysis was realized on a EuroVector EA-3000 instrument. TLC was performed using Polychrom SI F254 plates. Melting points of all synthesized compounds were determined with a Hanon Instruments automatic melting point apparatus MP450 in open capillary tubes.

According to the HPLC MS data, all synthesized compounds are > 95 % pure. All solvents and reagents were commercial grade and, if required, purified in accordance with the standard procedures. Starting unsaturated ketones were synthesized as described in [35].

*General procedures for the preparation of substituted 3-hydroxy-2-(phenyl)-4H-chromen-4-ones (1–14).*

*Method A ("linear" method).* Substituted 1-(2-hydroxyphenyl)-3-phenylprop-2-en-1-one (10 mmol) was dissolved in methanol (100 mL) at RT, 1.2 mL 50 % solution of potassium hydroxide was added to reaction mixture and 1.5 mL 30 % solution of $H_2O_2$ was added at stirring. The mixture was heated at 50°C for 10 min and the mixture was acidification to pH 2–3. After cooling, the solid was filtered, washed by water and dried at RT.

*Method B (one-pot method).* 2-Hydroxyacetophenone (40 mmol) and corresponding aldehyde (40 mmol) were dissolved in methanol (100 mL) at 50°C and 3 mL 50 % solution of potassium hydroxide was added to reaction mixture. The mixture was heated at 35°C for 24 h. At RT 1.5 mL 30 % solution of $H_2O_2$ was added at stirring. The mixture was heated at 50°C for 10 min and the mixture was acidification to pH 2–3. The solid was filtered, washed by water and dried at RT.

*3-Hydroxy-2-(4-carboxyphenyl)-4H-chromen-4-one (7).* 3-Hydroxy-2-(4-carboxyphenyl)-4H-chromen-4-one (7) was obtained by Method A. Yield 1.35 g (48 %), yellow solid, mp > 220°C (with decomp., from ethanol). $^1$H NMR spectrum, δ, ppm: 13.27 (bs, 1H, COOH), 9.98 (s, 1H, OH), 8.36 (d, 2H, Ar), 8.14 (τ, 1H, Ar), 8.12 (d, 2H, Ar), 7.81 (dd, 2H, Ar), 7.50 (t, 1H, Ar). $^{13}$C NMR spectrum, δ, ppm: 173.2, 166.18, 154.7, 143.9, 140.0, 134.4, 134.1, 129.8, 127.6, 125.3, 124.7, 121.3, 118.5. Mass spectrum, *m/z* ($I_{rel}$, %): 283.0 $[M+H]^+$(100). Found, %: C 68.12; H 3.59. $C_{16}H_{10}O_5$. Calculated, %: C 68.09; H 3.57.

*3-Hydroxy-2-(4-fluorophenyl)-4H-chromen-4-one (9).* 3-Hydroxy-2-(4-fluorophenyl)-4H-chromen-4-one (9) was obtained by Method A. Yield 1.41 g (55 %), yellow solid, mp 151–152°C (from ethanol). $^1$H NMR spectrum, δ, ppm: 9.70 (s, 1H, OH), 8.27 (dd, 2H, Ar), 8.10 (d, 1H, Ar), 7.81–7.73 (m, 2H, Ar), 7.46 (t, 1H, Ar), 7.40 (t, 2H, Ar). $^{13}$C NMR spectrum, δ, ppm: 172.9, 163.6, 161.6, 154.5, 144.4, 138.8, 133.7, 130.1, 124.6, 121.3, 118.4, 115.6. Mass spectrum, *m/z* ($I_{rel}$, %): 257.2 $[M+H]^+$(100). Found, %: C 70.27; H 3.56. $C_{15}H_9FO_3$. Calculated, %: C 70.31; H 3.54.

β-Glucosidase (β-D-glucoside glucohydrolase) from almonds were purchased from Sigma-Aldrich as lyophilized powder with > 98 % purity.

*Spectroscopic measurements.* Absorption spectra were recorded by Agilent Cary 3500 UV-Vis Multicell Spectrophotometer. Fluorescence was measured using a Hitachi 850 steady-state fluorescence spectrometer

equipped with double- grating excitation and emission monochromators. The fluorescence measurements were made in the phosphate buffer pH 7.4 (100 mM) in a 10×10 mm cuvette maintained at 20°C.

*Molecular docking setup*. The preparation of the receptor and ligands were carried out with the AutoDock Tools (ADT) software, version 1.5.7 [36]. The addition of hydrogen, the calculation of the Gasteiger charges of the receptor and ligands were also performed using the ADT software. Molecular docking calculations were carried out with the AutoDock Vina 1.1.2 software [37]. The 3D X-ray structure of *Paenibacillus polymyxa* β-glucosidase B (BglB, PDB ID: 2O9R) [38], *Raucaffricine* β-glucosidase (PDB ID: 4A3Y) [39] and human cytosolic β-glucosidase (hCBG, PDB ID: 2JFE) [40] were downloaded from the RCSB Protein Data Bank. The analysis of the protein structure was carried out using MolProbity [41].

We carried out the semi-flexible docking, so that the receptor was kept rigid and the ligand molecules were conformational flexible. The size of the cubic box generated by the ADT software, in the region of the receptor interaction (residues Glu167 and Glu356 for pBG, Glu186 and Glu420 for rBG and Glu165 and Glu373 for hBG, was defined as 65×65×65 Å. The center of the grid box was set at Cartesian coordinates $x = 61.980$, $y = 31.109$ and $z = 40.606$ for pBG, $x = 16.753$, $y = 23.943$ and $z = 41.579$ for rBG, $x = 38.208$, $y = 43.888$ and $z = 32.468$ for hBG with the grid point spacing set to 0.375 Å, respectively. For all runs, the number of binding modes was set to 9 and the exhaustiveness to 64. For each ligand, three independent runs were performed using different random seeds. The best docking mode corresponds to the largest ligand-binding affinity. Molecular graphics and visualization were performed using VMD 1.9.3 [42].

## 3. Results and discussion

Despite the wide use of flavonols in biomedical applications, their solubility is known to be very low in water, being about (0.12, 0.5, and < 0.01) $g \cdot L^{-1}$ at 20°C for rutin, naringin, and quercetin, respectively [43]. Therefore, to estimate the water solubility of the studied flavonols we calculated their logP using various approaches as summarized in Table 1. As can be seen from Table 1, the log*P* values estimated for the known natural flavonols are within a range of 1.3–3.0. These data can now be compared with the log*P* values of our synthetic flavonols 1–12, which were calculated to be in a range of 2.7–4.0, suggesting some lower solubility of these derivatives as compared to quercetin. It should also be noted that compounds 13–14 revealed the largest logP values of 4.8–6.2, which correlate with their very low water solubility.

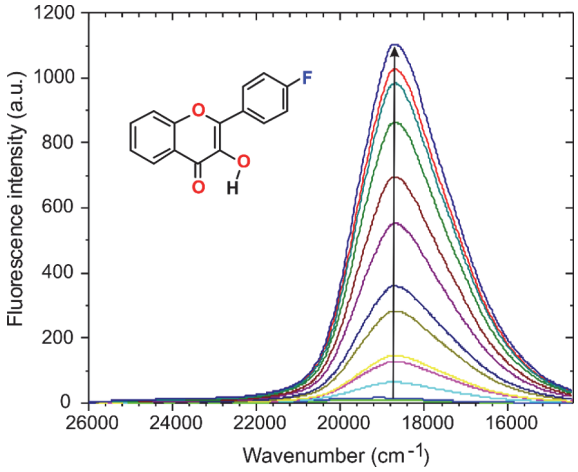


Fig. 2. Fluorescence titration of flavonol 9 with β-glucosidase in sodium phosphate buffer pH 7.4. The fluorescence was excited at 360 nm. The arrow corresponds to increase in the fluorescence intensity of flavonol 9 upon the increase in β-glucosidase concentration. The concentration of flavanol 9 was kept fixed at $2 \cdot 10^{-5}$ mol/l, whereas the β-glucosidase concentration was varied in a range from $0.5 \cdot 10^{-5}$ mol/l up to $14.6 \cdot 10^{-5}$ mol/l, respectively.

*Fluorescence titration*

We studied fluorescence properties of flavonols 7 and 9 in phosphate buffer at pH 7.4 in the presence and in the absence of β-glucosidase. The flavonols were added into the buffer as aliquot of their stocks in acetonitrile solution. An example of typical changes in emission spectra of flavonol 9 in the buffer solution as a function of concentration of β-glucosidase is shown in Fig. 2.

The fluorescence enhancement of flavonol 9 upon β-glucosidase titration was observed, which is characteristic of the protein-induced "turn-on" effect. These spectral changes of 9 are indicative of binding of a fluorophore with the protein, when the flavonol probe leaves polar aqueous solution and enters a nonpolar hydrophobic environment inside a protein pocket. Therefore, the loss of water-induced fluorescence quenching inside a protein are thought to be due to

Table 1. Physicochemical parameters of the studied and natural flavonols

| Compound | $M_w$, g/mol | log $P$[a] | | | | | |
|---|---|---|---|---|---|---|---|
| | | 1[a] | 2[b] | 3[c] | 4[d] | 5[e] | Average |
| 1 | 238.2 | 3.04 | 2.70 | 3.45 | 3.40 | 3.76 | 3.23 |
| 2 | 268.3 | 2.99 | 2.66 | 3.50 | 3.37 | 3.67 | 3.19 |
| 3 | 254.2 | 2.41 | 2.28 | 2.97 | 3.05 | 2.98 | 2.70 |
| 4 | 283.2 | 2.83 | 2.71 | 3.40 | 3.23 | 3.49 | 3.10 |
| 5 | 281.3 | 3.23 | 2.88 | 3.55 | 3.52 | 3.87 | 3.38 |
| 6 | 296.3 | 3.05 | 2.63 | 3.62 | 3.25 | 3.73 | 3.20 |
| 7 | 282.3 | 2.82 | 2.60 | 3.36 | 2.93 | 3.43 | 2.99 |
| 8 | 263.3 | 2.52 | 2.47 | 3.20 | 3.12 | 3.19 | 2.86 |
| 9 | 256.2 | 3.21 | 2.85 | 3.61 | 3.50 | 3.81 | 3.36 |
| 10 | 272.7 | 3.78 | 3.37 | 4.12 | 4.03 | 4.35 | 3.90 |
| 11 | 317.1 | 3.93 | 3.49 | 4.25 | 4.09 | 4.53 | 4.03 |
| 12 | 364.1 | 4.19 | 3.23 | 4.53 | 4.05 | 4.79 | 4.08 |
| 13 | 344.4 | 4.76 | 4.27 | 5.10 | 4.87 | 5.33 | 4.84 |
| 14 | 450.4 | 6.25 | 5.88 | 6.28 | 5.96 | 6.80 | 6.22 |
| Combretol | 388.4 | 2.87 | 2.47 | 3.09 | 3.44 | 2.62 | 2.86 |
| Morin | 302.2 | 1.13 | 1.47 | 1.88 | 1.54 | 1.61 | 1.48 |
| Myricetin | 318.2 | 0.83 | 1.72 | 1.39 | 1.18 | 2.11 | 1.31 |
| Ombuin | 303.3 | 3.07 | 2.38 | 2.83 | 2.52 | 2.92 | 2.72 |
| Quercetin | 302.2 | 1.50 | 1.71 | 1.68 | 1.54 | 2.07 | 1.68 |
| Retusin | 358.3 | 3.23 | 2.52 | 3.11 | 3.47 | 2.86 | 3.00 |

a — Calculated by ChemDraw 20.0
b — Calculated by PreADME [44]
c — Calculated by Molinspiration (https://www.molinspiration.com/)
d — Calculated by XLOGP3 [45]

deep penetration of flavonol 9 into the hydrophobic, water-free region of the β- glucosidase enzyme.

Similar changes in the emission behavior were also observed for flavonol 7 upon the increase in β-glucosidase concentration as shown in Fig. 3. Although flavonol 7 demonstrates (unlike flavonol 9) phototautomer fluorescence in aqueous medium, a penetration of this flavonol into the hydrophobic region of the β-glucosidase also results in the increase of the fluorescence intensity.

It can be seen that the emission band of flavonol 7 has a short-wavelength shoulder at about 470 nm. This shoulder is due to the emission of an anion form of the flavonol. The structure of this anion and the mechanism of its formation in the presence of β-glucosidase are going to be examined in our upcoming study. It is also worth to note that the anion formation is typical also for flavonol 9. However, since the absorption bands of the anion 9 are red-shifted relatively those of the anion 7, the anion fluorescence of 9 is not seen in Fig. 2 and ap-

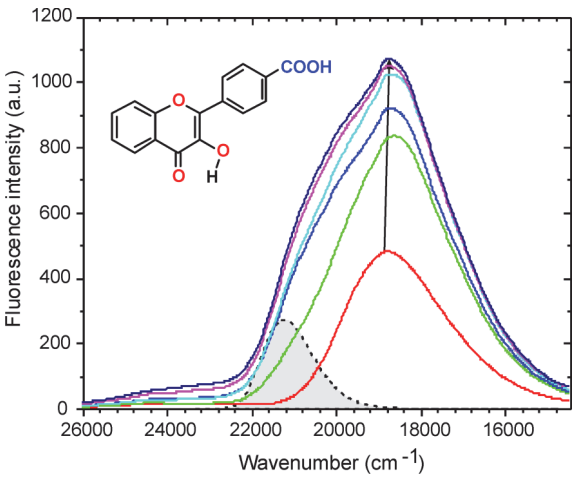


Fig. 3. Fluorescence titration of flavonol 7 with β-glucosidase in sodium phosphate buffer pH 7.4. The fluorescence was excited at 360 nm. The arrow corresponds to increase in the fluorescence intensity of 7 upon the increase in β-glucosidase concentration. The fluorescence of anionic form of 7 is shown by a dotted line as a shaded area.

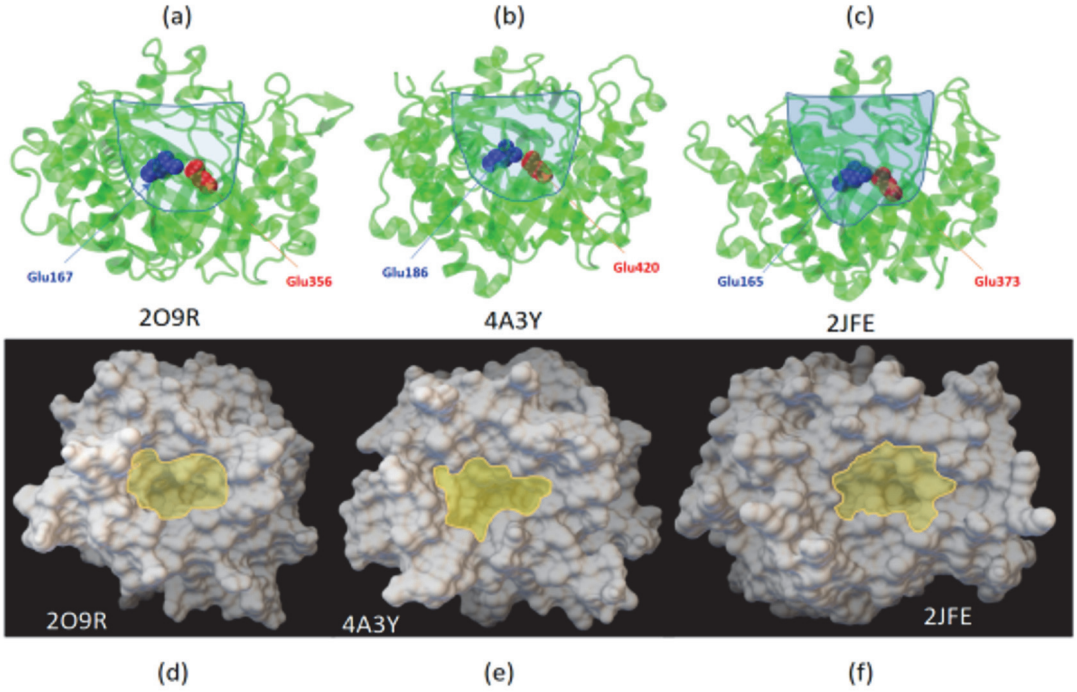


Fig. 4. X-ray structures of β-glucosidase from various sources: (a,d) from *Paenibacillus polymyxa* (BglB, PDB 2O9R), (b,e) from *Raucaffricine* (PDB 4A3Y), (c,f) human cytosol (PDB 2JFE). The active site Glu residues are labelled by blue and red. The active site pocket is schematically shown as blue (top panel a–c) and yellow (bottom panel d–f) shaded areas.

pears only after excitation in the long-wavelength region of the absorption spectrum.

*Molecular docking of some flavonols with β-glucosidase*

β-Glucosidase family includes enzymes with different activities widely distributed among all sort of living organisms, which are capable of the common ability to hydrolyse β-glycosidic linkages of disaccharides, oligosaccharides or conjugated saccharides [46]. Among the members of this family are bacterial and fungal cellobiases that play an essential role in cellulolytic hydrolysis [47]. Therefore, to study flavonol-protein interactions and to carry out molecular docking analysis, we used β-glucosidase enzymes for various sources. Although the alignment of β-glucosidase enzymes revealed sequence identity of 35–55 % only along its members from various sources, the detailed characterization of the atomic interactions at the aglycone site revealed a recognition pattern common to all bacterial β-glucosidases [38, 40, 47–48].

The high-resolution 3D structure of commercial β-glucosidase derived from Almonds are currently not available. Therefore, to elucidate of flavonol-protein interactions at the molecular level, we carried out molecular docking towards β-glucosidases taken from various sources, as summarized in Fig. 4. β-Glucosidases from *Paenibacillus polymyxa* (BglB), *Raucaffricine*, and human cytosol bear some common features. (i) All three enzymes have deep hydrophobic pocket capable of accommodation of substrate molecules during cellulolytic hydrolysis (Fig. 4a–f). (ii) The active site center is composed of two glutamate residues placed at close proximity one another (Fig. 4a–c).

We found that all studied flavonols were able to insert into a central cavity of β-glucosidase. The binding affinity towards β-glucosidase depends on the nature of peripheral substituents R and $R_1$ located in the 4‘-aryl ring of the flavonols, as well as on the structure of the β-glucosidase enzyme. Molecular docking results of the studied flavonols are summarized in Table 2. We found that the binding affinity of our synthetic flavonols 1–12 varies in a range from –8.2 up to –9.6 kcal/mol. The etherification of the peripheral hydroxyl groups in the 4‘-aryl moiety with the hydrophobic benzyl substituent significantly increase the affinity of the flavonols 13–14

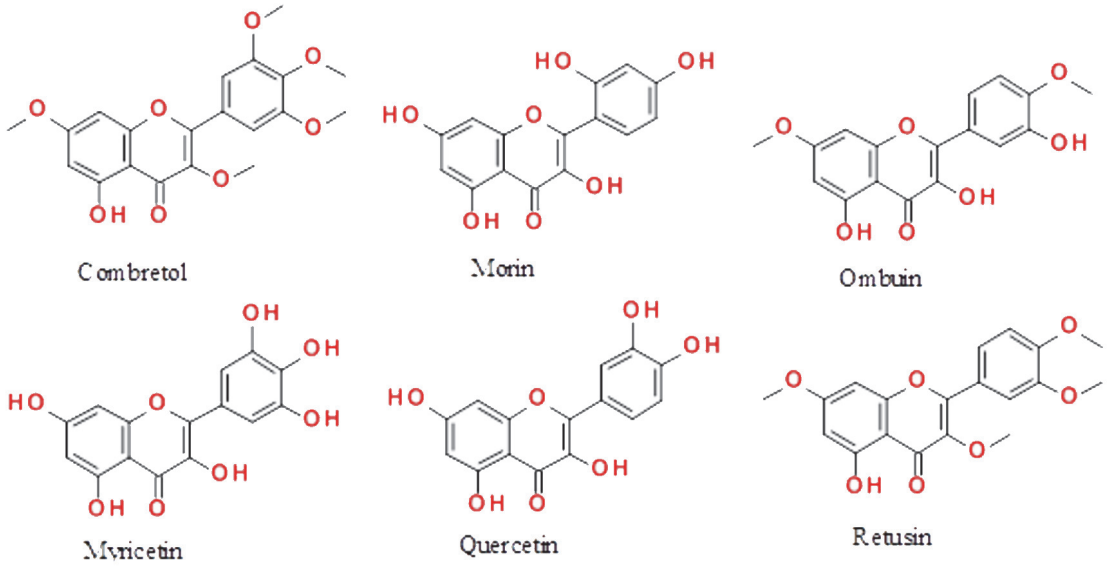


Fig. 5. Some natural flavonols revealing inhibitory activity towards glucosidase enzymes.

towards the β-glucosidase enzymes, so that the binding affinity increases up to –11.73 kcal/mol (Table 2).

The binding affinity of the studied flavonols may be compared with some well-known natural flavonols, such as combretol, morin [49–50], myricetin [50–51], ombuin, quercetin [49, 51] and retusin (Fig. 5), which have been studied in context of their inhibitory activity against various glucosidases by using experimental and computational techniques. For comparison reason, we carried out re-docking of the selected natural flavonols towards the same set of the β-glucosidase receptors and using the same molecular docking settings. The comparison of the binding affinity of these natural flavonols with the molecular docking results of our synthetic flavonols is given in Table 2. As can be noticed, the binding interaction energies of the most of our single-substituted synthetic flavonols 1–12 are the same order of the magnitude as their natural analogs. Moreover, some flavonols, such as 4 and 7, revealed the higher affinity in comparison with the known-natural analogues (Table 2).

*Paenibacillus polymyxa* β-glucosidase B (BglB). BglB enzyme has deep hydrophobic pocket with the active site located at the bottom of this pocket (about 16 Å deep) (Fig. 6a). The two catalytic glutamate residues, namely, the acid/base Glu167 and the nucleophile Glu356, are located deep within the active site. The BglB 3D structure (PDB 2O9R) has been used as a target for molecular docking calculations to identify inhibitors of its activity [52].

Figure 6 shows the binding mode of flavonol 9 toward Paenibacillus polymyxa β-glucosidase B. The molecular docking suggests that flavonol 9 inserts deeply into the hydrophobic cavity of BglB, as seen in Fig. 6a. The ligand binding is driven by hydrophobic interactions with aromatic Trp123, Trp328, Trp402, Trp410, Trp412 as well as residues Tyr169 and Tyr298, respectively. Moreover, the receptor-bound ligand 9 shields the active site residues Glu167 and Glu356 and may restrict accessibility of substrate molecules, which hold promise of the high inhibitory potency for this compound.

The binding mode of flavonol 7 towards BglB enzyme was found to be similar in many aspects to that of ligand 9. Figure 7 summarizes the binding interaction of flavonol 7 with BglB protein. As in the case of ligand 9, flavonol 7 also inserts deeply into the hydrophobic cavity of BglB, which agrees with the strong "turn-on" effect observed in the fluorescence titration experiments (Fig. 3).

*Raucaffricine* β-glucosidase. In Raucaffricine β-glucosidase enzyme, the two catalytic glutamate residues are Glu186 and Glu420, respectively (Fig. 3b). The enzyme X-ray 3D structure has been resolved at the high resolution of 2.5 Å (PDB 4A3Y) and, therefore, it has become a good target for molecular docking calculations [53–56]. Our docking study revealed that both flavonols 7 and 9 bind deeply inside the protein cavity.

Table 2. Molecular docking binding affinity of the synthetic and natural flavonols towards β-glucosidases from various sources

| Flanonol | Binding affinity, kcal/mol | | |
|---|---|---|---|
| | Human cytosolic β-glucosidase (PDB:2JFE) | *Paenibacillus polymyxa* β-glucosidase (PDB:2O9R) | *Raucaffricine* β-glucosidase (PDB:4A3Y) |
| 1 | −8.90 | −8.20 | −8.70 |
| 2 | −8.70 | −8.30 | −8.87 |
| 3 | −8.60 | −8.60 | −8.83 |
| 4 | −9.43 | −9.07 | −9.20 |
| 5 | −9.03 | −8.40 | −8.50 |
| 6 | −9.63 | −8.90 | −9.20 |
| 7 | −9.37 | −9.30 | −9.20 |
| 8 | −9.50 | −9.00 | −8.87 |
| 9 | −9.00 | −8.50 | −9.10 |
| 10 | −9.07 | −8.40 | −8.60 |
| 11 | −8.80 | −8.20 | −8.50 |
| 12 | −8.50 | −7.93 | −8.50 |
| 13 | −10.40 | −8.97 | −9.20 |
| 14 | −11.73 | −11.00 | −9.60 |
| Combretol | −7.77 | −8.13 | −7.43 |
| Morin | −8.60 | −8.63 | −8.90 |
| Myricetin | −8.77 | −8.87 | −9.10 |
| Ombuin | −8.13 | −8.47 | −8.80 |
| Quercetin | −8.97 | −8.90 | −9.00 |
| Retusin | −7.97 | −8.20 | −7.93 |

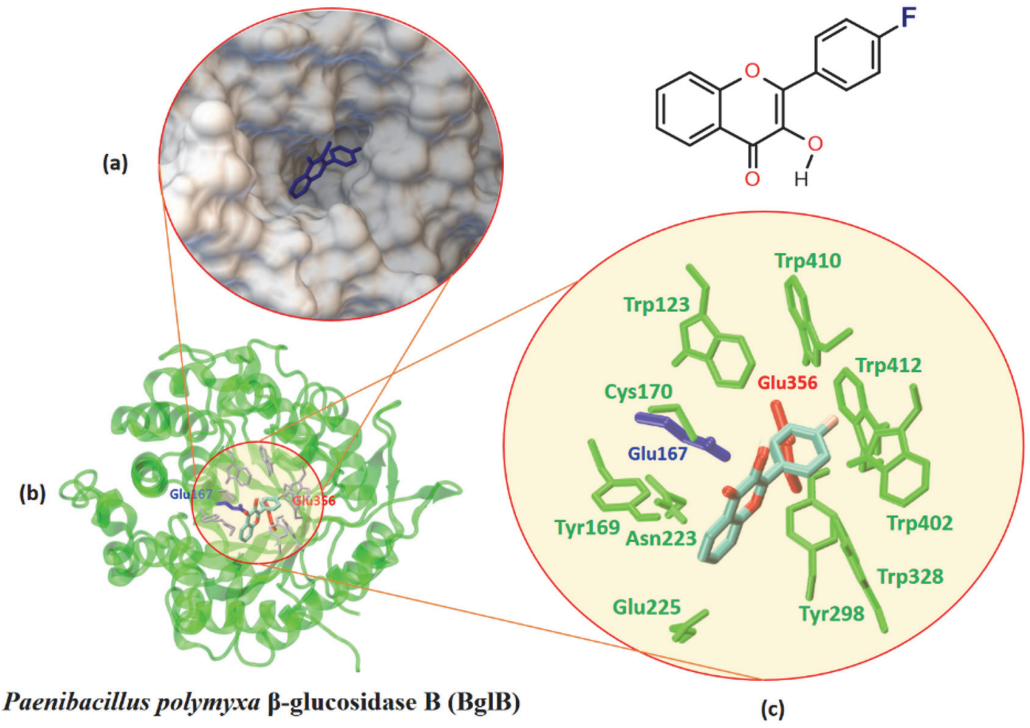


Fig. 6. The best docking pose of flavonol 9 at *Paenibacillus polymyxa* β-glucosidase B (BglB) (PDB code 2O9R). The enzyme is shown as a ribbon model at side (a) and (b) top views and ligand 9 is represented as a licorice model. The β-glucosidase active site residues Glu167 and Glu356 of are shown as blue and red sticks. An insert outlines ligand?protein interactions of flavonol 9 with the neighboring enzyme residues.

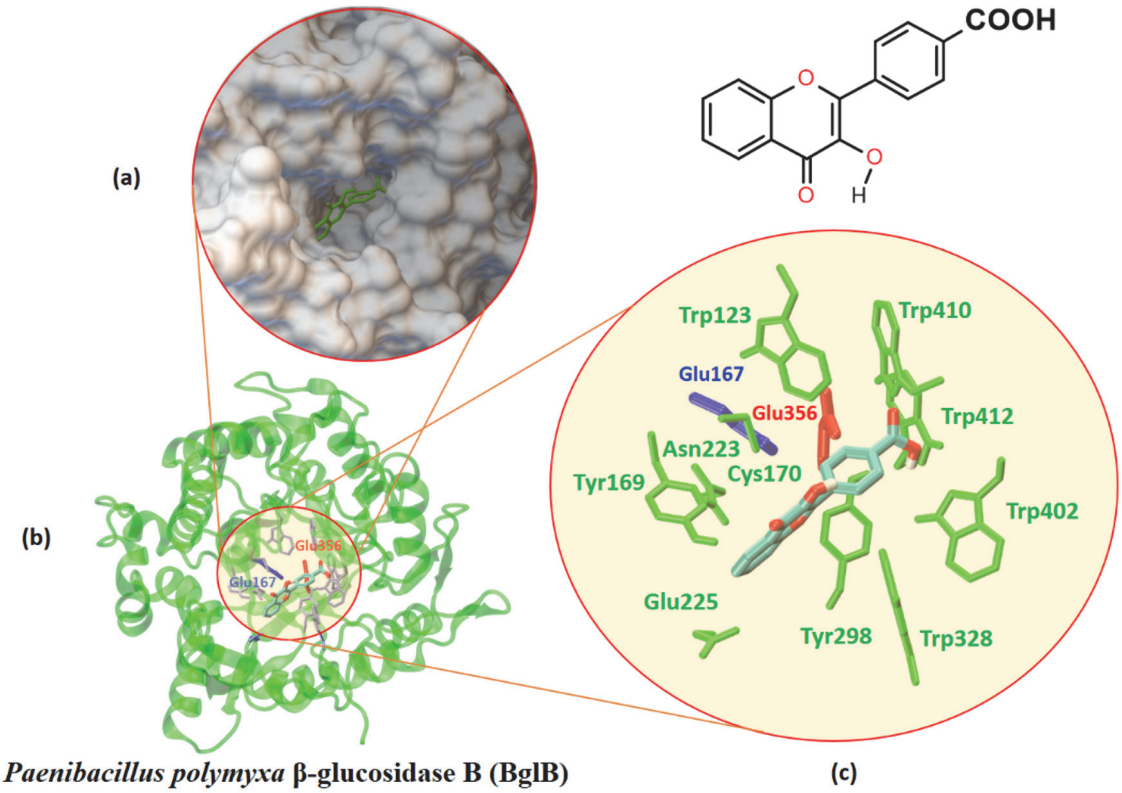


Fig. 7. The best docking pose of flavonol 7 at *Paenibacillus polymyxa* β-glucosidase B (BglB) (PDB code 2O9R). The enzyme is shown as a ribbon model at side (a) and (b) top views and ligand 7 is represented as a licorice model. The β-glucosidase active site residues Glu167 and Glu356 of are shown as blue and red sticks. An insert outlines ligand?protein interactions of flavonol 7 with the neighboring enzyme residues.

*Human cytosolic β-glucosidase (hCBG).* As other studied β-glucosidases, hCBG contains a deep hydrophobic protein pocket (Fig. 4c) with the two catalytic glutamates Glu165 and Glu373 located deep within this active site [40]. The hCBG 3D structure (PDB 2JFE) is well-resolved and used as a target for the molecular docking calculation [57]. Our molecular docking calculations suggest that all studied synthetic and natural flavonols bind strongly with the hCBG protein, so that the ligand molecule penetrate deeply inside the protein pocket. The binding energy and insertion mode reveal weak dependence on the flavonol structure (Table 2).

## 4. Summary and perspectives

In summary, we report the example of flavonol-based probes for fluorescence sensing of β-glucosidase in physiological solution. We observed that 4'-fluoro- and 4'-carboxyflavonols enhance their fluorescence upon the increase in the β-glucosidase concentration. The fluorescence intensity increase is up to 72-fold, which is indicative of the strong protein-induced "turn-on" effect. These data suggest that the studied flavonols favor binding to the protein, leaving polar aqueous solution and penetrating deep inside the nonpolar hydrophobic protein pocket of β-glucosidase enzyme. To identify favorable binding modes and the binding affinity of the synthetic flavonols towards β-glucosidases, we supplemented our fluorescence studied by molecular docking calculations. Molecular docking of a series of the synthesized flavonols and well-known natural analogs towards the high-resolution 3D structures of β-glucosidase enzyme taken from various sources revealed the high binding affinity varied from −8.2 kcal/mol up to −11.7 kcal/mol, respectively. All studied flavonols favor binding deeply inside the active pocket of the enzyme. The binding affinities are the same order of magnitude as for the well-known natural flavonols, which hold promise for the high inhibitory activity of the synthe-

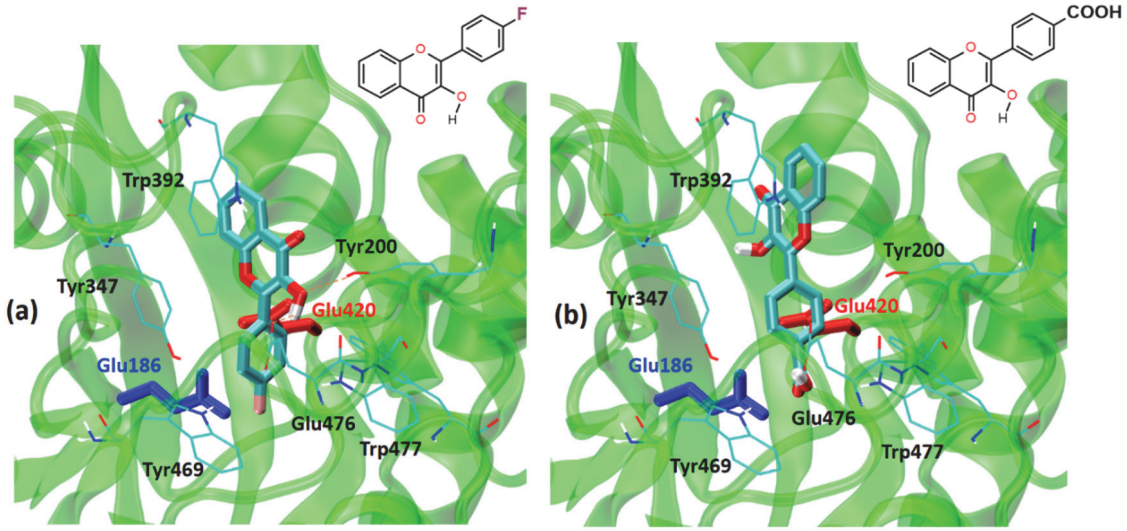


Fig. 8. The best docking pose of flavonol 9 (Panel a) and 7 (Panel a) bound to *Raucaffricine* β-glucosidase (PDB code 4A3Y). The enzyme is shown as a ribbon model and the ligands are represented as a licorice model. The active site residues Glu186 and Glu420 of β-glucosidase are shown as blue and red sticks.

sized flavonols against the enzymes from the glucosidase family. Moreover, our study suggest that the flavonol dyes can be a promising scaffold for the development of novel flavonol glycosides as easy-to-use "turn-on/off" fluorescent indicators of β-glucosidase activity in solution.

*Acknowledgments.* E.S.G., A.V.K., A.D.R. acknowledge Grant 2020.02/0016 "Indicators based on chromone derivatives for fluorescent determination of β-glucosidase activity" from the National Research Foundation of Ukraine.

## *References*

1. I.E.Serdiuk, A.D.Roshal, *Dyes and Pigments*, **138**, 223 (2017). http://dx.doi.org/10.1016/j.dyepig.2016.11.028.
2. A.S.Klymchenko, *Acc. Chem. Res.*, **50**, 366 (2017). https://doi.org/10.1021/acs.accounts.6b00517.
3. S.Hofener, P.C.Kooijman, J.Groen et al., *Phys. Chem. Chem. Phys.*, **15**, 12572 (2013). https://doi.org/10.1039/C3CP44267E.
4. A.Y.Chumak, V.O.Mudrak, V.M.Kotlyar, A.O.Doroshenko, *J. Photochem. Photobiol. A*, **406**, 112978 (2021). https://doi.org/10.1016/j.jphotochem.2020.112978.
5. Z.Xu, X.Zhao, M.Zhou et al., *Sens. Actuators. B*, **345**, 130367 (2021). https://doi.org/10.1016/j.snb.2021.130367.
6. T.Qin, B.Liu, Y.Huang et al., *Sens. Actuators. B*, **277**, 484 (2018). https://doi.org/10.1016/j.snb.2018.09.056.
7. T.Qin, B.Liu, Z.Xu et al., *Sens. Actuators, B*, **336**, 129718 (2021). https://doi.org/10.1016/j.snb.2021.129718.
8. X.Bi, B.Liu, L.McDonald et al., *J. Phys. Chem. B*, **121**, 4981 (2017). https://doi.org/10.1021/acs.jpcb.7b01885.
9. D.McDonald, M.Kasha, *J. Phys. Chem.*, **88**, 2235 (1984). https://doi.org/10.1021/j150655a012.
10. A.D.Roshal, J.A.Organero, A.Douhal, *Chem. Phys. Lett.*, **379**, 53 (2003). https://doi.org/10.1016/j.cplett.2003.08.008
11. I.E.Serdiuk, A.D.Roshal, *RSC Adv.*, **5**, 102191 (2015). https://doi.org/10.1039/C5RA13912K.
12. A.O.Doroshenko, A.V.Kyrychenko, O.M.Valyashko et al., *J. Photochem. Photobiol. A*, **383**, art. no. 111964 (2019). https://doi.org/10.1016/j.jphotochem.2019.111964.
13. A.P.Demchenko, S.Ercelen, A.D.Roshal, A.S.Klymchenko, *Polish J. Chem.*, **76**, 1287 (2002).
14. V.F.Valuk, G.Duportail, V.G.Pivovarenko, *J. Photochem. Photobiol.*, **175**, 226 (2005). https://doi.org/10.1016/j.jphotochem.2005.05.003.
15. X.Poteau, G.Saroja, C.Spies, R.G.Brown, *J. Photochem. Photobio*, **162**, 431 (2004). https://doi.org/10.1016/s1010-6030(03)00429-5.
16. W.Liu, Y.Wang, W.Jin et al., *J. Photochem. Photobio*, **383**, 299 (1999). https://doi.org/10.1016/s0003-2670(98)00789-2.
17. X.Jin, X.Sun, X.Di et al., *Sens. Actuators, B*, **224**, 209 (2016). https://doi.org/10.1016/j.snb.2015.09.072

18. A.D.Roshal, A.V.Grigorovich, A.O.Doroshenko et al., *J. Phys. Chem. A*, **102**, 5907 (1998). https://doi.org/10.1021/jp972519w.
19. A.D.Roshal, T.V.Sakhno, A.A.Verezubova et al., *Funct. Mater.*, **10**, 419 (2003).
20. A.Munoz, A.D.Roshal, S.Richelme et al., *Russ. J. Gen. Chem.*, **74**, 438 (2004). https://doi.org/10.1023/B:RUGC.0000030403.41976.5c.
21. B.Liu, Y.Pang, R.Bouhenni et al., *Chem. Commun.*, **51**, 11060 (2015). https://doi.org/10.1039/C5CC03516C.
22. K.A.Bertman, C.S.Abeywickrama, H.J.Baumann et al., *J. Mater. Chem. B*, **6**, 5050 (2018). https://doi.org/10.1039/C8TB00325D.
23. K.A.Bertman, C.S.Abeywickrama, A.Ingle et al., *J. Fluoresc.*, **29**, 599 (2019). https://doi.org/10.1007/s10895-019-02371-7.
24. S.Concilio, M.Di Martino, A.M.Nardiello et al., *Molecules*, **25**, 3458 (2020). https://doi.org/10.3390/molecules25153458.
25. L.McDonald, B.Liu, A.Taraboletti et al., *J. Mater. Chem. B*, **4**, 7902 (2016). https://doi.org/10.1039/C6TB02456D.
26. B.Liu, J.Wang, G.Zhang et al., *ACS Appl. Mater. Inter.*, **6**, 4402 (2014). https://doi.org/10.1021/am500102s.
27. B.Liu, L.McDonald, Q.Liu et al., *Sens. Actuators, B*, **235**, 309 (2016). https://doi.org/10.1016/j.snb.2016.05.079
28. I.E.Serdiuk, M.Reszka, H.Myszka et al., *RSC Adv.*, **6**, 42532 (2016). https://doi.org/10.1039/C6RA06062E.
29. A.T.Adetunji, F.B.Lewu, R.Mulidzi, B.Ncube, *J. Soil Plant Nutr.*, **17**, 794 (2017).
30. L.L.Escamilla-Trevino, W.Chen, M.L.Card et al., *Phytochem.*, **67**, 1651 (2006). https://doi.org/10.1016/j.phytochem.2006.05.022
31. A.V.Morant, K.Jorgensen, C.Jorgensen et al., *Phytochem.*, **69**, 1795 (2008). https://doi.org/10.1016/j.phytochem.2008.03.006
32. T.D.Butters, *Curr Opin Struct Biol.*, **11**, 412 (2007). https://doi.org/10.1016/j.cbpa.2007.05.035
33. X.Zhou, Z.Huang, H.Yang et al., *Biomed Pharmacotherapy*, **91**, 504 (2017). https://doi.org/10.1016/j.biopha.2017.04.113
34. M.A.Smith, R.M.Neumann, R.A.Webb, *J. Heterocycl. Chem.*, **5**, 425 (1968). https://doi.org/10.1002/jhet.5570050323
35. Z.Qiang, W.Chun, L.Yunping et al., *Chin. J. Appl. Environ. Biol.*, **23**, 232 (2017). https://doi.org/10.3724/SP.J.1145.2016.04019.
36. D.S.Goodsell, G.M.Morris, A.J.Olson, *J. Mol. Recognit.*, **9**, 1 (1996). https://doi.org/10.1002/(SICI)1099-1352(199601)9:1::AID-JMR2413.0.CO;2-6
37. O.Trott, A.J.Olson, *J. Comput. Chem.*, **31**, 455 (2010). https://doi.org/10.1002/jcc.21334
38. P.Isorna, J.Polaina, L.Latorre-Garcia et al., *J. Mol. Biol.*, **371**, 1204 (2007). https://doi.org/10.1016/j.jmb.2007.05.082
39. L.Xia, M.Ruppert, M.Wang, *ACS Chem. Biol.*, **7**, 226 (2012). https://doi.org/10.1021/cb200267w
40. S.Tribolo, J.-G.Berrin, P.A.Kroon, *J. Mol. Biol.*, **370**, 964 (2007). https://doi.org/10.1016/j.jmb.2007.05.034
41. C.J.Williams, J.J.Headd, N.W.Moriarty et al., *Prot. Sci.*, **27**, 293 (2018). doi:https://doi.org/10.1002/pro.3330
42. W.Humphrey, A.Dalke, K.Schulten, *J.Mol. Graphics*, **14**, 33 (1996). doi: 10.1016/0263-7855(96)00018-5
43. L.Chebil, C.Humeau, J.Anthoni et al., *Chem. Eng. Data*, **52**, 1552 (2007), https://doi.org/10.1021/je7001094
44. S.K.Lee, I.H.Lee, H.J.Kim et al., *EuroQSAR 2002 Designing Drugs and Crop Protectants: Processes, Problems and Solutions (2003), p.418. doi:*
45. T.Cheng, Y.Zhao, X.Li et al., *J. Chem. Inf. Model.*, **47**, 2140 (2007). https://doi.org/10.1021/ci700257y
46. Y.Bhatia, S.Mishra, V.S.Bisaria, *Crit. Rev. Biotech.*, **22**, 375 (2002). https://doi.org/10.1080/07388550290789568.
47. J.R.Ketudat Cairns, B.Mahong, S.Baiya, J.-S.Jeon, *Plant Sci.*, **241**, 246 (2015). doi: https://doi.org/10.1016/j.plantsci.2015.10.014
48. S.He, S.G.Withers, ????????, **272**, 24864 (1997). https://doi.org/10.1074/jbc.272.40.24864.
49. C.Proenca, M.Freitas, D.Ribeiro et al., *J. Enzyme Inhib. Med. Chem.*, **32**, 1216 (2017). https://doi.org/10.1080/14756366.2017.1368503
50. L.Zeng, G.Zhang, S.Lin, D.Gong, *J. Agric. Food Chem.*, **64**, 6939 (2016). https://doi.org/10.1021/acs.jafc.6b02314.
51. K.Tadera, Y.Minami, K.Takamatsu, T.I.Matsuoka, *J. Nutrition. Sci. Vitaminology*, **52**, 149 (2006). https://doi.org/10.3177/jnsv.52.149.
52. T.A.Ajayeoba, J.O.Woods, A.O..Ayeni, *J. Mol. Struct.*, **1237**, 130275 (2021). https://doi.org/10.1016/j.molstruc.2021.130275
53. G.-Y.Chen, H.Zhang, F.-Q.Yang, *Analyt. Chim. Actav*, **1142**, 19 (2021). https://doi.org/10.1016/j.aca.2020.10.047
54. M.Kazmi, S.Zaib, A.Ibrar et al., *Bioorg. Chem.*, **77**, 190 (2018). https://doi.org/10.1016/ j.bioorg.2017.12.022
55. S.Riaz, I.U.Khan, M.Yar et al., *J. Bioorg. Chem.*, **57**, 148 (2014). https://doi.org/10.1016/j.bioorg.2014.10.007
56. A.D.Snizhko, A.V.Kyrychenko, E.S.Gladkov, *Int. J. Mol. Sci.*, **23**, 3781 (2022).
57. S.Khan, T.Pozzo, M.Megyeri et al., *BMC Biochem.*, **12**, 11 (2011). https://doi.org/10.1186/1471-2091-12-11